

# High Poisson's ratio of Earth's inner core explained by carbon alloying

C. Prescher<sup>1,2\*</sup>, L. Dubrovinsky<sup>1</sup>, E. Bykova<sup>1,3</sup>, I. Kuppenko<sup>1,4</sup>, K. Glazyrin<sup>1,5</sup>, A. Kantor<sup>1,4</sup>, C. McCammon<sup>1</sup>, M. Mookherjee<sup>1,6</sup>, Y. Nakajima<sup>1,7</sup>, N. Miyajima<sup>1</sup>, R. Sinmyo<sup>1</sup>, V. Cerantola<sup>1</sup>, N. Dubrovinskaia<sup>3</sup>, V. Prakapenka<sup>2</sup>, R. Rüffer<sup>4</sup>, A. Chumakov<sup>4,8</sup> and M. Hanfland<sup>4</sup>

**Geochemical, cosmochemical, geophysical, and mineral physics data suggest that iron (or iron-nickel alloy) is the main component of the Earth's core<sup>1-3</sup>. The inconsistency between the density of pure iron at pressure and temperature conditions of the Earth's core and seismological observations can be explained by the presence of light elements<sup>1,4</sup>. However, the low shear wave velocity and high Poisson's ratio of the Earth's core remain enigmatic<sup>2</sup>. Here we experimentally investigate the effect of carbon on the elastic properties of iron at high pressures and temperatures and report a high-pressure orthorhombic phase of iron carbide, Fe<sub>7</sub>C<sub>3</sub>. We determined the crystal structure of the material at ambient conditions and investigated its stability and behaviour at pressures up to 205 GPa and temperatures above 3,700 K using single-crystal and powder X-ray diffraction, Mössbauer spectroscopy, and nuclear inelastic scattering. Estimated shear wave and compressional wave velocities show that Fe<sub>7</sub>C<sub>3</sub> exhibits a lower shear wave velocity than pure iron and a Poisson's ratio similar to that of the Earth's inner core. We suggest that carbon alloying significantly modifies the properties of iron at extreme conditions to approach the elastic behaviour of rubber. Thus, the presence of carbon may explain the anomalous elastic properties of the Earth's core.**

The density of pure iron at high pressures and temperatures has been reported to be 3 to 10% higher than the density of the Earth's outer core<sup>5</sup> and 2.5 to 9% denser than its inner core<sup>3,6</sup> at the relevant pressure and temperature conditions. The magnitude of the discrepancy between mineral physics data and seismological observations<sup>1,2</sup> is strongly dependent on the chosen thermal profile of the Earth. Several light elements, including hydrogen, carbon, oxygen, silicon and sulphur, have been proposed as either the sole or primary component(s) that could alloy with iron under conditions corresponding to the Earth's core. Although recent experimental studies on the compressional wave velocities of light-element-bearing iron alloys can explain both geophysical observations and satisfy geochemical constraints<sup>4,7,8</sup>, none have been able to successfully account for the anomalously low shear wave velocity and the high Poisson's ratio in the Earth's inner core. Neither can partial melting of the outer layer of the Earth's inner core<sup>9</sup> explain the high Poisson's ratio, which is practically uniform throughout the entire inner core. Furthermore, extrapolation of existing mineral physics data on pure iron and iron alloys containing nickel, silicon or

hydrogen to Earth's inner-core pressure and temperature conditions shows Poisson's ratios between 0.32 and 0.385 (refs 10–14), whereas according to seismological data<sup>2</sup> the Poisson's ratio of the Earth's inner core is about 0.44. In fact, this high value is close to the maximum possible Poisson's ratio of 0.5, which characterizes the elastic properties, for example, of rubber. Thus, the alloying component(s) needs to modify the elastic properties of iron to such an extent that at pressures above 330 GPa and several thousands of degrees the alloy exhibits elastic properties similar to rubber or lead (0.4–0.45) at ambient conditions.

We explored the effect of carbon on the elastic properties of iron at high pressures and temperatures. It is already known that at moderate pressures (below 60 GPa) one of the iron carbide phases, Fe<sub>3</sub>C, exhibits relatively low shear velocity<sup>15,16</sup> and even in its non-magnetic phase shows only a limited decrease of compressibility with increasing pressure<sup>17</sup>. Moreover, carbon is a plausible light element in the Earth's core<sup>18</sup> and estimates based on current available data suggest that 1.1 wt% of carbon may be present in the Earth's inner core<sup>18</sup>. Although studies of iron–carbon alloys are challenging owing to experimental difficulties in controlling their chemical purity at extreme pressures and temperatures, investigation of intermetallic compounds has been shown to provide strong mineralogical constraints on the geochemistry and properties of the Earth's core<sup>4</sup>.

We conducted multi-anvil experiments in the Fe–C system at pressures between 7 and 15 GPa and temperatures between 1,473 and 1,973 K. In all experiments the stoichiometry of iron carbide determined by microprobe analysis was Fe<sub>7</sub>C<sub>3</sub>, in good agreement with previous investigations<sup>19–22</sup>. However, single-crystal X-ray diffraction (SCXRD) of the synthesized materials indicates an orthorhombic symmetry with space group *Pbca* (Fig. 1 and Supplementary Fig. 1), in contrast to previously reported hexagonal *P6<sub>3</sub>mc* (ref. 23) and orthorhombic *Pnma* (ref. 24) polytypes. This orthorhombic structure (*Pbca* space group) is previously unknown for iron carbides. Hereafter the material will be further referred to as o-Fe<sub>7</sub>C<sub>3</sub>. Both previously reported structures of Fe<sub>7</sub>C<sub>3</sub> were proposed based on powder diffraction data, whereas the structure reported in this work was solved from single-crystal diffraction data. Considering the ambiguity in solving complex structures based on powder diffraction data, definitive proof of the existence of the previously described structures with *P6<sub>3</sub>mc* and *Pnma* space groups is still lacking. The only previous single-crystal X-ray

<sup>1</sup>Bayerisches Geoinstitut, Universität Bayreuth, 95440 Bayreuth, Germany. <sup>2</sup>Center for Advanced Radiation Sources, University of Chicago, Chicago, Illinois 60637, USA. <sup>3</sup>Laboratory of Crystallography, Material Physics and Technology at Extreme Conditions, University of Bayreuth, D-95440 Bayreuth, Germany. <sup>4</sup>European Synchrotron Radiation Facility (ESRF), F-38043 Grenoble Cedex, France. <sup>5</sup>Petra III, P02, Deutsches Elektronen Synchrotron, 22607 Hamburg, Germany. <sup>6</sup>Earth and Atmospheric Sciences, Cornell University, Ithaca, New York 14853, USA. <sup>7</sup>Materials Dynamics Laboratory, RIKEN Spring-8 Center, Hyogo 679-5148, Japan. <sup>8</sup>National Research Center "Kurchatov Institut", Moscow 123182, Russia. \*e-mail: clemens.prescher@gmail.com

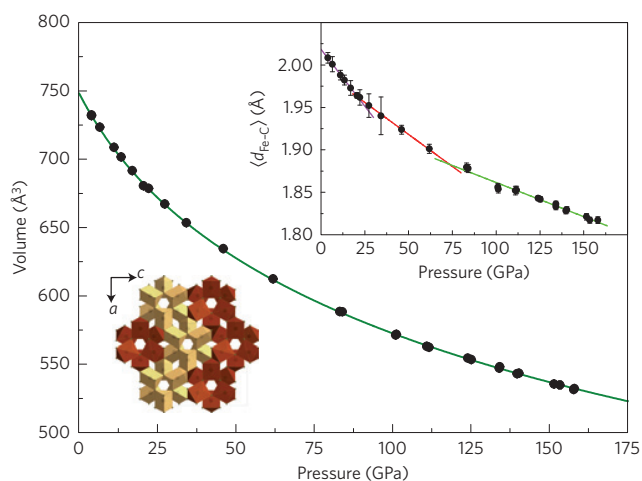


**Figure 1 | Volume-pressure data for  $o\text{-Fe}_7\text{C}_3$  with the fitted third-order Birch-Murnaghan equation of state ( $K_{300} = 168(4)$  GPa,  $K' = 6.1(1)$ ). The upper inset shows the variation of mean carbon to iron distances, ( $d_{\text{Fe-C}}$ ), in  $o\text{-Fe}_7\text{C}_3$  with pressure, whereby the data show three linear regions with transitions around 16 GPa and 70 GPa, marking the ferromagnetic to paramagnetic and paramagnetic to non-magnetic transitions, respectively (further details are given in the text). The lower left inset shows a polyhedral model of the crystal structure of  $o\text{-Fe}_7\text{C}_3$  projected in the  $b$ -direction.**

diffraction investigation<sup>22</sup> of  $\text{Fe}_7\text{C}_3$  is based on data collected over a small omega range of  $\pm 13^\circ$ – $16^\circ$ , resulting in only 13–34 uniquely indexed reflections, thus making a definitive structure solution impossible. In contrast, we solved and refined the crystal structure of  $o\text{-Fe}_7\text{C}_3$  ( $Pbca$ , Supplementary Fig. 1c) based on 1,473 unique reflections (Supplementary Table 1). The structural units of  $o\text{-Fe}_7\text{C}_3$  are distorted  $\text{CFe}_6$  trigonal prisms with relatively short Fe–C distances (Fig. 1 and Supplementary Fig. 1 and Supplementary Table 2) varying from  $\sim 1.96$  to  $\sim 2.06$  Å. Three prisms are connected through shared vertices in triads. The triads are arranged in columns parallel to the  $b$  axis through shared vertices; in addition each triad is rotated by  $60^\circ$  relative to its neighbour. The columns may be oriented parallel or antiparallel to the  $b$ -axis. Columns connect with each other through the common edges of trigonal prisms; each column has six neighbours directed either antiparallel or parallel. The same structural type (atomic arrangement) has been observed for  $\text{Ca}_7\text{Au}_3$  (ref. 25), and there are obvious similarities with previously reported structures of  $\text{Fe}_7\text{C}_3$  (Supplementary Fig. 1).

To further explore the structural stability of  $o\text{-Fe}_7\text{C}_3$ , we conducted several laser-heated diamond anvil cell experiments at pressures up to 205 GPa and temperatures above 3,500 K (Supplementary Table 2). In all experiments the structure of the quenched and/or *in situ* (if studied) phase remained identical to that of the starting  $o\text{-Fe}_7\text{C}_3$  phase. Further, we melted  $o\text{-Fe}_7\text{C}_3$  (as indicated by the formation of a spherical blob) on heating at 180 GPa in a Ne pressure-transmitting medium. Transmission electron microscopy unambiguously confirmed that the recovered sample

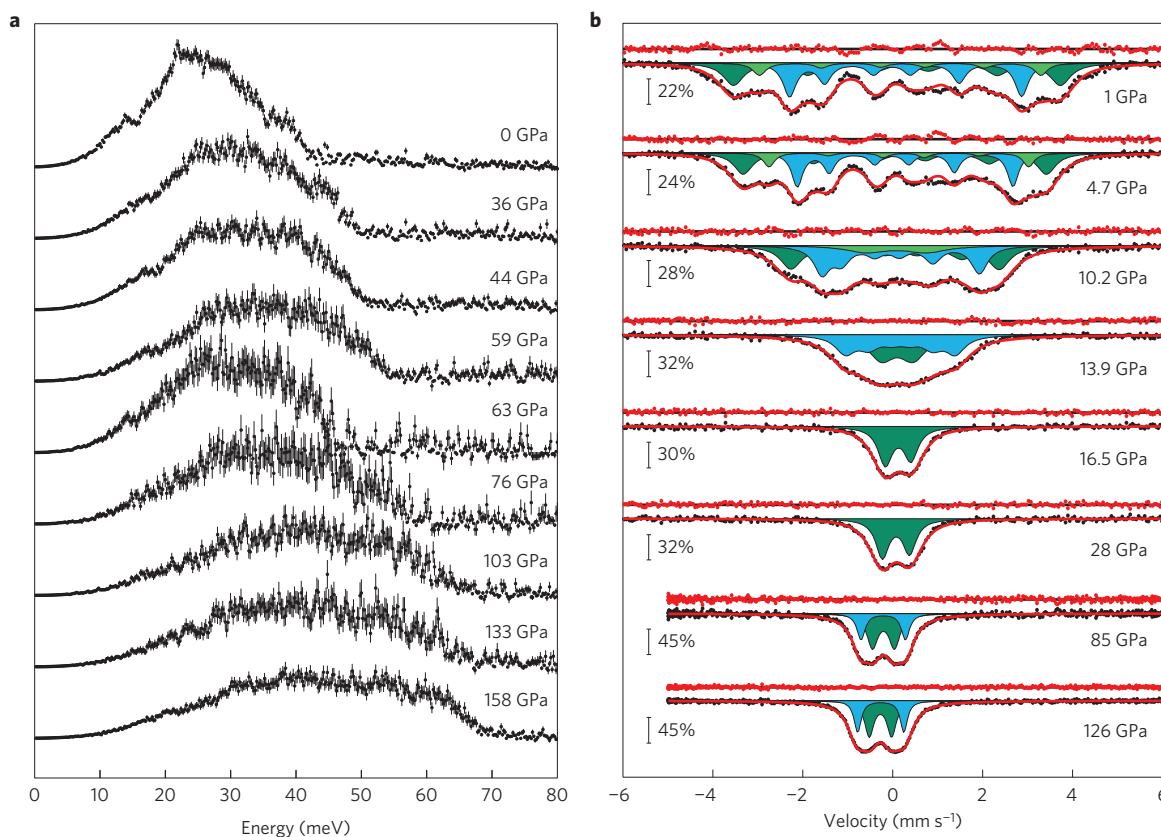


**Figure 2 | Nuclear resonance measurements of  $o\text{-Fe}_7\text{C}_3$  at high pressure. a**, Iron partial density of phonon states (pDOS) of  $o\text{-Fe}_7\text{C}_3$  at selected pressure points. The pDOS were extracted from NIS measurements at the respective pressures. **b**, Selected energy-domain SMS spectra of  $o\text{-Fe}_7\text{C}_3$  up to 126 GPa at room temperature, showing the transition between ferromagnetic sextets and a paramagnetic doublet around 16.5 GPa. Red lines show the theoretical fits as well as the residual (indicated above each spectrum) and the relative absorption is indicated by percentage bars. The spectra were fitted to the minimum number of components (shaded green and blue) needed for a statistically acceptable fit. The SMS spectra at 85 GPa and 126 GPa were collected with a higher energy resolution, enabling a fit of two paramagnetic doublets.

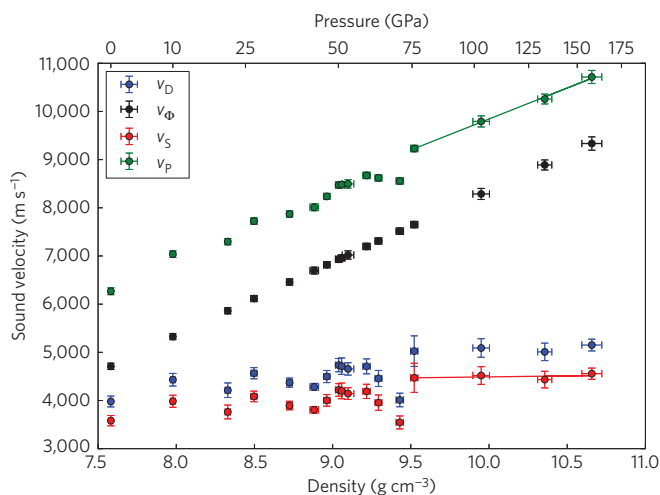


**Figure 3 |** Variation of Debye sound velocity  $v_D$ , bulk sound velocity  $v_\phi$ , shear wave velocity  $v_S$  and compressional wave velocity  $v_P$  of  $\text{Fe}_7\text{C}_3$  with density. Linear fits to the non-magnetic data for compressional (green) and shear wave (red) velocities were used to extrapolate sound wave velocities and Poisson's ratios to conditions of the Earth's inner core.

had the same structure as the starting material (Supplementary Fig. 3). The melting experiments demonstrate that o- $\text{Fe}_7\text{C}_3$  is the liquidus phase at conditions of the Earth's outer core. Hence, studying the behaviour of o- $\text{Fe}_7\text{C}_3$  at high pressures and temperatures is essential to understanding the effects of carbon alloying on the density and elastic properties of iron.

We further performed single-crystal X-ray diffraction (SCXRD) of o- $\text{Fe}_7\text{C}_3$  up to 158 GPa employing a diamond anvil cell and observed no structural phase transitions (Fig. 1 and Supplementary Tables 3 and 4). Even at the highest pressure reached we were able to collect 311 reflections ( $R_{\text{int}} = 5.4\%$ ) and refine the structure to  $R1 = 7.8\%$ . The  $P$ - $V$  data can be fitted by a single third-order Birch-Murnaghan equation of state with parameters of  $V_0 = 748(1) \text{ \AA}^3/\text{unit cell}$ ,  $K = 168(4) \text{ GPa}$ , and  $K' = 6.1(1)$  (Fig. 1). Our results do not indicate changes in the compressional behaviour, in contrast to the hexagonal h- $\text{Fe}_7\text{C}_3$  phase, which exhibits anomalous behaviour at around 53 GPa (ref. 23). The equation-of-state parameters suggest that o- $\text{Fe}_7\text{C}_3$  is as compressible as pure iron<sup>3</sup>. Although the  $P$ - $V$  data do not show discontinuities, changes in the compression behaviour of o- $\text{Fe}_7\text{C}_3$  are indicated by variations of the average C-Fe distances (Fig. 1 and Supplementary Fig. 4 and Supplementary Table 4), which exhibit three different linear regions, with changes in slopes occurring around 20 GPa and 70 GPa. Notably these pressures are close to previously predicted or reported electronic transitions in h- $\text{Fe}_7\text{C}_3$  (refs 21,22).

To understand these changes in the compression behaviour of o- $\text{Fe}_7\text{C}_3$ , we measured Mössbauer spectra up to 131 GPa, employing the newly developed energy-domain synchrotron Mössbauer source (SMS) at the nuclear resonance beamline (ID18; ref. 26) at the European Synchrotron Radiation Facility. A loss of ferromagnetism is marked by the disappearance of magnetic hyperfine splitting above 16 GPa (Fig. 2) and an abrupt change in the pressure variation of centre shift above 70 GPa indicates an electronic reconfiguration (Supplementary Fig. 5). The compression behaviour of o- $\text{Fe}_7\text{C}_3$  is similar to that of  $\text{Fe}_3\text{C}$  (ref. 17) and indicates that o- $\text{Fe}_7\text{C}_3$  exhibits a ferromagnetic to paramagnetic transition at 16 GPa and a paramagnetic to non-magnetic transition at 70 GPa. Both electronic transition pressures are in reasonable agreement with changes in the behaviour of the mean C-Fe distances on compression.

To follow the pressure dependence of the Poisson's ratio of o- $\text{Fe}_7\text{C}_3$  we investigated the vibrational and elastic properties of

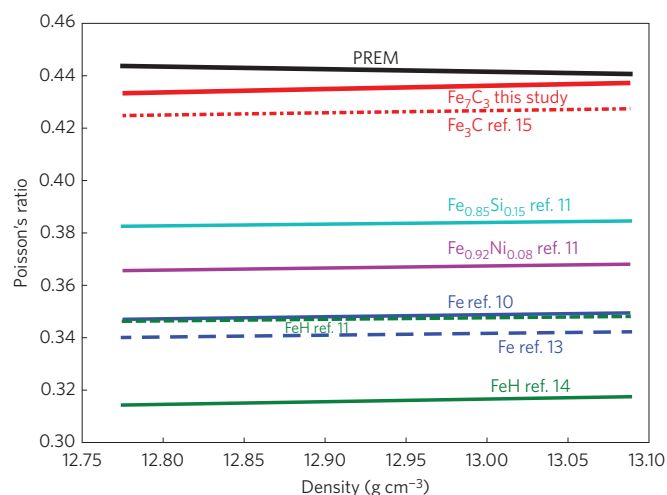


**Figure 4 |** Extrapolation of Poisson's ratio to the densities estimated in the Earth's inner core using Birch's law. The only element which significantly increases the Poisson's ratio of iron is carbon. Moreover, the estimated Poisson's ratio of  $\text{Fe}_7\text{C}_3$  nearly approaches the Poisson's ratio of the preliminary Earth reference model (PREM; ref. 2) at densities near the centre of the inner core.

the material up to  $\sim 158$  GPa using nuclear inelastic scattering (NIS). The partial  $^{57}\text{Fe}$  density of phonon states (pDOS) were extracted from the collected NIS spectra<sup>27</sup> (Fig. 2) and Debye sound velocities  $v_D$  were obtained from a linear fit to the low-energy region of the reduced pDOS (ref. 28; Supplementary Figs 6 and 7). Combining the estimated  $v_D$  with the equation-of-state parameters determined from the high-pressure SCXRD data enables the calculation of aggregate compressional wave velocity  $v_P$ , shear wave velocity  $v_S$  and Poisson's ratio  $\nu$ . The resulting values of  $v_D$  and  $v_S$  increase only slowly with increasing pressure and density and are nearly pressure invariant above the paramagnetic to non-magnetic transition around 70 GPa (Fig. 3); whereas  $v_P$  increases over the entire pressure range. Therefore the Poisson's ratio increases from 0.26(3) at ambient conditions to the remarkably high value of 0.39(3) at the highest pressure achieved (Supplementary Table 5). Furthermore, the paramagnetic to non-magnetic transition at 70 GPa is accompanied by a decrease in  $v_D$ , probably induced by a phonon softening due to the electronic transition.

To extrapolate sound wave velocities to conditions of the Earth's inner core ( $P > 330 \text{ GPa}$ ,  $T \sim 5,000 \text{ K}$ ) we employed Birch's law, where sound wave velocity scales linearly with density, independent of sample temperature (Fig. 3). Using the extrapolated sound wave velocities of the non-magnetic o- $\text{Fe}_7\text{C}_3$  phase we calculated the corresponding Poisson's ratios at the conditions of the Earth's inner core (Fig. 4). The Poisson's ratio of o- $\text{Fe}_7\text{C}_3$  approaches the high value of the Earth's inner core at the  $P$ - $T$  conditions at the centre of the Earth (0.44). The extrapolated high Poisson's ratio of o- $\text{Fe}_7\text{C}_3$  is a robust result that is obtained even if the complete data set, including ferromagnetic and paramagnetic o- $\text{Fe}_7\text{C}_3$ , is used for the extrapolation. Although the shear wave velocity increases with pressure in this case, the compressional wave velocity does also, and the resulting Poisson's ratio (0.42) is still very close to the value of the Earth's inner core. Although the validity of Birch's law has been challenged in the past decade and shear wave velocity was observed to decrease with increasing temperature at constant density<sup>16,29</sup>, the magnitude of this softening is debatable owing to neglecting the effect of electronic and topologic transitions in the studied materials,  $\text{Fe}_3\text{C}$  and iron, respectively, which were undiscovered at the time of those studies<sup>17,30</sup>. To investigate the effect of temperature on sound velocities of o- $\text{Fe}_7\text{C}_3$  we additionally collected high-temperature

NIS spectra using a double-sided laser-heated diamond anvil cell (Supplementary Table 3). The results show a small decrease of  $v_D$  and  $v_S$  with increasing temperature, whereas  $v_P$  remains nearly constant. Therefore, high temperatures will lead to even higher Poisson's ratios of o-Fe<sub>7</sub>C<sub>3</sub>. Although we do not yet have sufficient data to quantitatively constrain  $v_D$  at high  $P$ - $T$  conditions, existing measurements suggest that data at 300 K already provide a lower bound for estimates, and further studies at high temperatures will probably strengthen our conclusions.

Our results present a convincing argument for carbon as an important component of Earth's core<sup>18–20</sup>, and show in addition that carbon alloying can drastically change the elastic properties of iron, thus explaining the anomalously high Poisson's ratio of the Earth's inner core.

## Methods

The final complete structural solution of o-Fe<sub>7</sub>C<sub>3</sub> was obtained from single crystals synthesized at 18 GPa and 1,773 K using a four-circle Oxford Diffraction Xcalibur diffractometer ( $\lambda = 0.7107$  Å) equipped with an Xcalibur Sapphire2 CCD detector. Single-crystal high-pressure diamond anvil cell experiments were conducted at beamline ID09a at the European Synchrotron Radiation Facility (ESRF). Diffraction data were collected at 293 K using a MAR555 flatpanel detector, radiation with a wavelength of 0.4149 Å and a beam size of  $10 \times 10 \mu\text{m}^2$ .

High-temperature and high-pressure powder X-ray diffraction measurements were conducted at the GSECARS 13-ID-D beamline at the Advanced Photon Source (ANL) using double-sided laser heating, a MARCCD detector, radiation with a wavelength of 0.3344 Å and a beam size of  $3 \times 4 \mu\text{m}^2$ . Transmission electron microscopy analysis of the quenched molten sample was performed using a Philips CM20 field-emission gun system (FEG) operated at 200 kV.

<sup>57</sup>Fe-enriched Fe<sub>7</sub>C<sub>3</sub> powder was synthesized for nuclear inelastic scattering (NIS) and synchrotron Mössbauer source (SMS) spectroscopy at the same conditions of 18 GPa and 1,773 K as for the single crystals. Energy-domain SMS measurements were performed at the nuclear resonance beamline (ID18) at ESRF. The velocity scale was calibrated relative to a 25- $\mu\text{m}$ -thick natural  $\alpha$ -Fe foil and centre shift values are given relative to  $\alpha$ -Fe. The source line width was measured before and after each sample measurement using K<sub>2</sub>Mg<sup>57</sup>Fe(CN)<sub>6</sub>.

NIS measurements were performed on the nuclear resonance beamline (ID18) at ESRF. The focused X-ray beam was less than 10  $\mu\text{m}$  in diameter and has an energy resolution of 0.7 meV. Two avalanche photodiodes were used to collect the inelastic scattering signal perpendicular to the synchrotron X-ray beam. NIS spectra were collected over a range of  $-20$  to 80 meV around the <sup>57</sup>Fe nuclear resonance energy in steps of 0.2 meV.

Detailed descriptions of methods and any associated references are available in the Supplementary Information.

Received 14 October 2014; accepted 20 January 2015;  
published online 23 February 2015

## References

- Birch, F. Elasticity and constitution of the Earth's interior. *J. Geophys. Res.* **57**, 227–286 (1952).
- Dziewonski, A. M. & Anderson, D. L. Preliminary reference Earth model. *Phys. Earth Planet. Inter.* **25**, 297–356 (1981).
- Dubrovinsky, L. S., Saxena, S. K., Tutti, F., Rekhi, S. & LeBehan, T. *In situ* X-Ray study of thermal expansion and phase transition of iron at multimegabar pressure. *Phys. Rev. Lett.* **84**, 1720–1723 (2000).
- Badro, J. *et al.* Effect of light elements on the sound velocities in solid iron: Implications for the composition of Earth's core. *Earth Planet. Sci. Lett.* **254**, 233–238 (2007).
- Anderson, O. L. & Isaak, D. G. Another look at the core density deficit of Earth's outer core. *Phys. Earth Planet. Inter.* **131**, 19–27 (2002).
- Dewaele, A. *et al.* Quasihydrostatic equation of state of iron above 2 Mbar. *Phys. Rev. Lett.* **97**, 215504 (2006).
- Antonangeli, D. *et al.* Composition of the Earth's inner core from high-pressure sound velocity measurements in Fe–Ni–Si alloys. *Earth Planet. Sci. Lett.* **295**, 292–296 (2010).
- Mao, Z. *et al.* Sound velocities of Fe and Fe–Si alloy in the Earth's core. *Proc. Natl Acad. Sci. USA* **109**, 10239–10244 (2012).
- Gubbins, D., Sreenivasan, B., Mound, J. & Rost, S. Melting of the Earth's inner core. *Nature* **473**, 361–363 (2011).
- Mao, H. K. *et al.* Phonon density of states of iron up to 153 gigapascals. *Science* **292**, 914–916 (2001).

- Lin, J.-F. *et al.* Sound velocities of iron–nickel and iron–silicon alloys at high pressures. *Geophys. Res. Lett.* **30**, 2112 (2003).
- Mao, W. L. *et al.* Nuclear resonant X-ray scattering of iron hydride at high pressure. *Geophys. Res. Lett.* **31**, L15618 (2004).
- Murphy, C. A., Jackson, J. M. & Sturhahn, W. Experimental constraints on the thermodynamics and sound velocities of hcp-Fe to core pressures. *J. Geophys. Res.* **B 118**, 1999–2016 (2013).
- Shibasaki, Y. *et al.* Sound velocity measurements in dhcp-FeH up to 70 GPa with inelastic X-ray scattering: Implications for the composition of the Earth's core. *Earth Planet. Sci. Lett.* **313–314**, 79–85 (2012).
- Gao, L. *et al.* Pressure-induced magnetic transition and sound velocities of Fe<sub>3</sub>C: Implications for carbon in the Earth's inner core. *Geophys. Res. Lett.* **35**, 1–5 (2008).
- Gao, L. *et al.* Effect of temperature on sound velocities of compressed Fe<sub>3</sub>C, a candidate component of the Earth's inner core. *Earth Planet. Sci. Lett.* **309**, 213–220 (2011).
- Prescher, C. *et al.* Structurally hidden magnetic transitions in Fe<sub>3</sub>C at high pressures. *Phys. Rev. B* **85**, 6–9 (2012).
- Wood, B. J., Li, J. & Shahar, A. Carbon in the core: Its influence on the properties of core and mantle. *Rev. Mineral Geochem.* **75**, 231–250 (2013).
- Nakajima, Y., Takahashi, E., Suzuki, T. & Funakoshi, K. "Carbon in the core" revisited. *Phys. Earth Planet. Inter.* **174**, 202–211 (2009).
- Lord, O. T., Walter, M. J., Dasgupta, R., Walker, D. & Clark, S. M. Melting in the Fe–C system to 70 GPa. *Earth Planet. Sci. Lett.* **284**, 157–167 (2009).
- Mookherjee, M. *et al.* High-pressure behavior of iron carbide (Fe<sub>3</sub>C) at inner core conditions. *J. Geophys. Res.* **116**, B04201 (2011).
- Chen, B. *et al.* Magneto-elastic coupling in compressed Fe<sub>7</sub>C<sub>3</sub> supports carbon in Earth's inner core. *Geophys. Res. Lett.* **39**, 2–5 (2012).
- Herbstein, F. H. & Snyman, J. A. Identification of Eckstrom–Adcock iron carbide as Fe<sub>7</sub>C<sub>3</sub>. *Inorg. Chem.* **3**, 894–896 (1964).
- Fruchart, R. & Rouault, A. Sur l'existence de macles dans les carbures orthorhombiques isomorphes Cr<sub>7</sub>C<sub>3</sub>, Mn<sub>7</sub>C<sub>3</sub>, Fe<sub>7</sub>C<sub>3</sub>. *Ann. Chim.* **4**, 143–145 (1969).
- Fornasini, M. L. & Merlo, F. Ca<sub>7</sub>Au<sub>3</sub> and Ca<sub>5</sub>Au<sub>4</sub>, two structures closely related to the Th<sub>7</sub>Fe<sub>3</sub> and Pu<sub>3</sub>Rh<sub>4</sub> types. *J. Solid State Chem.* **59**, 65–70 (1985).
- Potapkin, V. *et al.* The <sup>57</sup>Fe synchrotron Mössbauer source at the ESRF. *J. Synchrotr. Radiat.* **19**, 559–569 (2012).
- Chumakov, A. & Rüffer, R. Nuclear inelastic scattering. *Hyperf. Interact.* **113**, 59–79 (1998).
- Achterhold, K. *et al.* Vibrational dynamics of myoglobin determined by the phonon-assisted Mössbauer effect. *Phys. Rev. E* **65**, 051916 (2002).
- Lin, J.-F. *et al.* Sound velocities of hot dense iron: Birch's law revisited. *Science* **308**, 1892–1894 (2005).
- Glazyrin, K. *et al.* Importance of correlation effects in hcp iron revealed by a pressure-induced electronic topological transition. *Phys. Rev. Lett.* **110**, 117206 (2013).

## Acknowledgements

Partial financial support was provided through the German Science Foundation (DFG), the German Ministry of Education and Research (BMBF), and the PROCOPE exchange programme. We acknowledge the European Synchrotron Radiation Facility for provision of synchrotron radiation facilities through both the normal user programme and a Long Term Project. Portions of this work were performed at GeoSoilEnviroCARS (Sector 13), Advanced Photon Source (APS), Argonne National Laboratory. GeoSoilEnviroCARS is supported by the National Science Foundation—Earth Sciences (EAR-1128799) and Department of Energy—Geosciences (DE-FG02-94ER14466). Use of the Advanced Photon Source was supported by the US Department of Energy, Office of Science, Office of Basic Energy Sciences, under Contract No. DE-AC02-06CH11357.

## Author contributions

M.M. and Y.N. synthesized the starting materials. E.B., K.G., N.D., L.D. and M.H. performed the SCXRD measurements. C.P., L.D., C.M., I.K., A.K., M.M., R.S., V.C., R.R. and A.C. performed the NIS measurements. C.P., L.D. and V.P. performed the high-pressure, high-temperature powder X-ray diffraction measurements. N.M. performed the TEM analysis of the recovered molten sample. C.P., L.D., K.G., I.K., A.K., A.C. and R.R. performed the SMS experiments. C.P., L.D., E.B. and C.M. performed the data analysis. C.P., L.D. and C.M. wrote the paper. All authors discussed the results and commented on the manuscript.

## Additional information

Supplementary information is available in the online version of the paper. Reprints and permissions information is available online at [www.nature.com/reprints](http://www.nature.com/reprints). Correspondence and requests for materials should be addressed to C.P.

## Competing financial interests

The authors declare no competing financial interests.